Preprints of the 19th World Congress
The International Federation of Automatic Control
Cape Town, South Africa. August 24-29, 2014

Nonlinear Model Based Fault Detection of Lithium Ion Battery Using Multiple Model Adaptive Estimation

Amardeep Singh*, Afshin Izadian, Sohel Anwar***

**Department of Mechanical Engineering, IUPUI, Indianapolis, IN 46202 USA (Tel: 317-274-7640; e-mail: soanwar@iupui.edu).*
*** Energy Systems and Power Electronics Laboratory, IUPUI, Indianapolis, IN 46202, USA (e-mail: aizadian@iupui.edu)*

Abstract: In this paper, an adaptive fault diagnosis technique is used for fault detection in Lithium ion batteries. The monitoring setup consists of multiple models representing the different degree of parameter shift due to over-discharge in the Lithium ion battery. A recursive least square estimator along with equivalent circuit methodology is used to construct the non-linear battery models. Extended Kalman filters are used to generate the estimated terminal voltages for each system. The residuals are further evaluated using the conditional probability evaluation function, to generate probabilities that determine the presence of a particular operational condition. Using experimental data, it is shown that Li-ion battery performance shift due to over-discharge can be accurately detected in real time.

1. INTRODUCTION

The battery technology of today has come a long way since its modest beginnings more than two centuries ago. The batteries in use today are smaller in size, with higher energy density, and have longer life with enhanced inherent safety (Tarascon and Armand, 2001). Batteries with lithium based chemistries have shown unprecedented increase in use over the last decade. The rechargeable Lithium-ion (Li-ion) batteries can be found in applications like mobile phones, cameras, critical applications like hybrid electric vehicles (HEV), electric vehicles (EV), and medical implants (Nagata et al., 2005). With the Li-ion battery available in various form factors, their application as a power source is extensive and wide spread. With increased use, it is imperative to ensure the safe operation of the Li-ion battery, which further leads to user safety. Failure in Li-ion batteries can be attributed in general to a combination of manufacturing defects, safety component failure, and/or human abuse. From the various fault scenarios, over discharge (OD) causes appreciable change in battery performance. In addition to being linked with capacity loss during cycling (Kanevskii and Dubasova, 2005), OD in extreme conditions can cause over heating of the battery, which further results in vaporization of active material and hence explosion. Repeated OD of the Li-ion battery causes slow variation in the battery performance over time, and if left unchecked, OD can lead to permanent, and in extreme conditions, catastrophic failure (Zhang and Lee, 2011).

Fault detection and diagnosis (FDD) in Li-ion batteries is a multidisciplinary research involving electrochemistry, controls, machine learning among others. Fault detection (FD) using control theory techniques, specifically state estimation, involves the evaluation of the state of the battery under test. While the choice of observer depends on the system and state, the objective is to access the critical information pertaining to Li-ion battery that is not readily available through measurement (Alavi et al., 2013). In (Chen et al., 2013), the authors use a bank of reduced order Luenberger observers (LO) for FDD in Li-ion batteries. In systems with little or no measurement noise, LO for FDD can be a good choice. With noise, as in the case of Li-ion measured parameters, the suggested setup will face inherent difficulties under subtle but important parameter variation. In presence of system and measurement noise, observer based fault diagnosis using Kalman filter shows good performance. In (Singh et al., in press), a bank of Kalman filters under the paradigm of multiple model adaptive estimation (MMAE) technique, an adaptive FDD method, along with impedance spectroscopy is used for accurate FDD in Li-ion batteries. Because of the associated disadvantages of impedance spectroscopy, namely expensive and bulky setup, delays in parameter extraction, this paper further develops the work in (Singh et al., in press), to implement system identification using recursive least squares (RLS) with MMAE for accurate detection of Li-ion battery performance degradation.

Real time implementation of battery fault detection dictates the use of a technique that is computationally inexpensive and yet captures the cell dynamics accurately. The equivalent circuit modelling technique (Xidong et al., 2011), is a good choice when it comes to system identification, observer based fault detection and minimal computational effort with good mapping to electrochemical phenomenon of the Li-ion battery.

The paper is organized as follows: section 2 describes the non-linear battery model, section 3 describes the RLS when applied to Li-ion battery model, and Section 4 covers the model based fault detection. Section 5 covers the state estimation and conditional probability generation. Design of experiments and the discussion of the results obtained are covered in sections 6 and 7 respectively.

2. BATTERY MODELING

The Li-ion battery is modelled as a third order system consists of lumped electrical elements like resistors, capacitors and voltage source. The simplified cell model is shown in Figure 1.

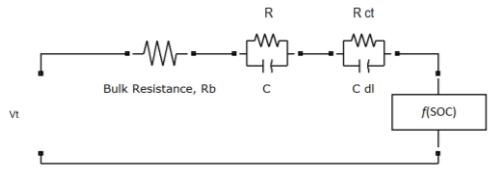

Fig. 1. Li-ion battery equivalent circuit model

The resistor R_b represents the bulk electrolyte resistance, constant phase element (CPE) given by capacitor C, and resistor R are used to model the distribution of reactivity depicting the local property of the electrode, charge transfer resistance R_{ct} and double layer capacitance C_{dl} represent the interfacial impedance of the cell (Orazem and Tribollet, 2008, Barsoukov and Macdonald, 2005), and *f(SOC)* represents the battery cell open circuit voltage (OCV) as a function of state of charge (SOC). The circuit parameters depend on the SOC, temperature and capacity fade effects (Buller et al., 2005). For this study, parameter dependency on these factors is assumed to be small. The effect of non-linear element in the equivalent circuit namely Warburg impedance representing the diffusion phenomenon is considered to be negligible (Kaypmaz and Tuncay, 2011).

The non-linearity in the system is primarily introduced by the OCV-SOC relationship for Li-ion battery, which is found experimentally (Abu-Sharkh and Doerffel, 2004). This relationship, given in Figure 2, was recorded for a sample $LiFePO_4$ battery cell operating at room temperature at the Energy Systems and Power Electronics Laboratory (ESPEL) at IUPUI. A ninth order polynomial given by (1) is fit to the OCV-SOC curve of Figure 2.

$$u(SOC) = a_9(SOC^{9}) + a_8(SOC^{8}) + a_7(SOC^{7}) + a_6(SOC^{6}) + a_5(SOC^{5}) + a_4(SOC^{4}) + a_3(SOC^{3}) + a_2(SOC^{2}) + a_1(SOC) + a_0 \quad (1)$$

$a_1 = 0.0385 a_2 = -0.01936 a_3 = -0.169 a_4 = 0.06142 a_5 = 0.2328 a_6 = -0.05715 a_7 = -0.08321 a_8 = 0.0005257 a_9 = 0.03205 a_{10} = 3.297$

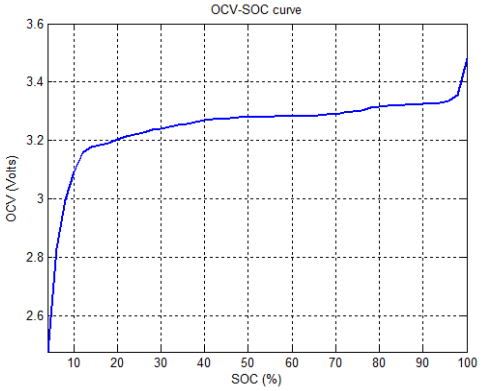

Fig. 2. OCV-SOC curve for $LiFEPO_4$

The SOC is defined as the ratio of the remaining capacity to the fully charged capacity of the battery (Ehsani et al., 2009) and is given by

$$SOC(t) = SOC(0) + \int_0^t \frac{\eta I_L(\tau)}{C_n} \quad (2)$$

where, *SOC(0)* is the initial SOC, η represents the coulomb efficiency given by $\eta = \begin{cases} 1, charging \\ 0.98, discharging \end{cases}$, I_L is the charge/discharge current in Ampere, and C_n represents the battery cell capacity in Ampere hour. The sign convention used in this study considers negative sign of I_L as discharging while positive sign as charging.

Using Kirchhoff's voltage law, the voltage across capacitor C is given by

$$\dot{V}_C = -\frac{V_C}{R \times C} + \frac{I_L}{C} \quad (3)$$

The voltage across the double layer capacitor is given by

$$\dot{V}_{Cdl} = -\frac{V_{Cdl}}{R_{ct} \times C_{dl}} + \frac{I_L}{C_{dl}} \quad (4)$$

The terminal voltage V_t is obtained from

$$V_t = u(SOC) - I_L R_b - V_C - V_{Cdl} \quad (5)$$

where $I_L R_b$ represents the voltage drop across the bulk resistance.

The discrete time version of (2) can be given as:

$$SOC(k) = SOC(k-1) + \frac{\eta I_L(k-1)T}{C_n} \quad (6)$$

where T is the sample time.

The discrete time counterparts of (3) and (4) can be obtained using zero-order hold (ZOH) (Ogata, 1995) as follows

$$V_C(k) = e^{-\frac{T}{R \times C}} V_C(k-1) + R\left(1 - e^{-\frac{T}{R \times C}}\right) I_L(k-1) \quad (7)$$

$$V_{Cdl}(k) = e^{-\frac{T}{R_{ct} \times C_{dl}}} V_{Cdl}(k-1) + R_{ct}\left(1 - e^{-\frac{T}{R_{ct} \times C_{dl}}}\right) I_L(k-1) \quad (8)$$

The state variable is given by $x(k) = [SOC(k) \quad V_C(k) \quad V_{Cdl}(k)]^T$ and the nonlinear battery model is given by

$$\begin{aligned} x(k) &= g(x(k-1), I_L(k-1)) + w(k-1) \\ z(k) &= h(x_k, I_L(k)) + v(k) \end{aligned} \quad (9)$$

where g and h are continuously differentiable nonlinear functions while w is the input noise with zero mean and covariance of

$$E\{w_n[l] w_n^T[m]\} = \begin{cases} Q, l = m \\ 0, l \neq m \end{cases} \quad (10)$$

and v is the measurement noise, independent from w, with zero mean value as

$$E\{v_n[l] v_n^T[m]\} = \begin{cases} R', l = m \\ 0, l \neq m \end{cases} \quad (11)$$

Q and R' are the process and measurement noise variances respectively. The process and measurement white Gaussian noise is generated using the polar method (Ross, 2010). Using (6), (7) and (8) the function g is given by

$$g(k-1)=\begin{bmatrix} SOC\ (k-1)+\dfrac{\eta I_L(k-1)T}{C_n} \\ e^{-\frac{T}{R\times C}}V_C(k-1)+R\left(1-e^{-\frac{T}{R\times C}}\right)I_L(k-1) \\ e^{-\frac{T}{R_{ct}\times C_{dl}}}V_{Cdl}(k-1)+R_{ct}\left(1-e^{-\frac{T}{R_{ct}\times C_{dl}}}\right)I_L(k-1) \end{bmatrix} \quad (12)$$

From (5) the function *h* is given by

$$h(k)=u(SOC)-I_L(k)R_b-V_C(k)-V_{Cdl}(k) \quad (13)$$

With different values for the circuit elements R_b, R, C, R_{ct} and C_{dl}; distinct models can be obtained each representing a signature fault or health of the battery cell.

3. SYSTEM IDENTIFICATION

The RLS method is a classical system identification technique and aims at fitting mathematical model to a sequence of observed data by minimizing the sum of the squares of the difference between the observed and computed data recursively (Ioannou and Fidan, 2006). The unknown parameter identification requires the system to be represented in discrete-time parametric form given by

$$z(k)=\theta^{*T}\ \phi(\mathrm{k}) \quad (14)$$

where *z(k)* is the system output, θ^* is a linear vector of unknown parameters and is being identified by RLS, $\phi(k)$ is the vector of earlier inputs and outputs. From (1) and (5), the terminal voltage is given by

$$\begin{aligned} V_t(k)=&\ a_9(SOC(k)^9)+a_8(SOC(k)^8)+a_7(SOC(k)^7)+ \\ &a_6(SOC(k)^6)+a_5(SOC(k)^5)+a_4(SOC(k)^4)+a_3(SOC(k)^3)+ \\ &a_2(SOC(k)^2)+a_1(SOC(k))+a_0-I_L(k)R_b-V_C(k)-V_{Cdl}(k) \end{aligned} \quad (15)$$

substituting (7) and (8) in (15) and separating the unknown parameters from the known signals, the parametric form for battery model is given by

$$V_t(k)=\begin{bmatrix} a_9 & \dots & a_0 & R_b & e^{-\frac{T}{R\times C}} & R\left(1-e^{-\frac{T}{R\times C}}\right) & e^{-\frac{T}{R_{ct}\times C_{dl}}} & R_{ct}\left(1-e^{-\frac{T}{R_{ct}\times C_{dl}}}\right) \end{bmatrix}^{*T}$$
$$\times\begin{bmatrix} SOC(k)^9 & \dots & SOC(k)^0 & -I_L(k) & -V_C(k-1) & -I_L(k-1) & -V_{Cdl}(k-1) & -I_L(k-1) \end{bmatrix} \quad (16)$$

for further simplification, the combined parameters can be represented as

$$A_1=e^{-\frac{T}{R\times C}},\ B_1=R\left(1-e^{-\frac{T}{R\times C}}\right),\ A_2=e^{-\frac{T}{R_{ct}\times C_{dl}}},\ B_2=R_{ct}\left(1-e^{-\frac{T}{R_{ct}\times C_{dl}}}\right)$$

The estimation equation is given by

$$\theta(k)=\theta(k-1)+P(k)\phi(k)\varepsilon(k) \quad (17)$$

at k=1, $\theta(0)$ is the best initial guess of parameters to be identified, P is the covariance matrix, ε is the normalized estimation error, and ϕ is from (14).

The normalized estimation error ε is given by

$$\varepsilon(k)=\frac{V_t(k)-\theta(k)^T\phi(k)}{m^2(k)} \quad (18)$$

where m^2 is the normalizing signal and is given by

$$m^2(k)=cc+\phi^T(k)\phi(k) \quad (19)$$

with *cc* as a positive scalar value.

The covariance matrix P is recursively updated by using the following equation

$$P(k)=P(k-1)-\frac{P(k-1)\phi(k)\phi^T(k)P(k-1)}{m^2(k)+\phi^T(k)P(k-1)\phi(k)} \quad (20)$$

with $P(0)=P_0={P_0}^T>0$.

The information regarding the condition of the battery is partially available in the OCV-SOC relationship and partially in the circuit parameters. OD alters the response of the battery while charging and discharging, and this information is used to observe and collect the variation in all the 15 parameters combined. Out of the 15 parameters, 10 are from the OCV-SOC relationship while 5 are from the equivalent circuit.

4. MODEL BASED FAULT DETECTION

The model based fault detection and fault diagnosis structure used in this paper is shown in Figure 3. As a special case of observer based fault diagnosis, MMAE uses a bank of non-linear Kalman filters to generate the residuals. Each filter represents a particular operational condition of the battery and has access to the present and past terminal voltage Vt and load/charging current I_L. The critical information carrying residuals are further deciphered using the condition probability density evaluator block to generate the conditional probabilities.

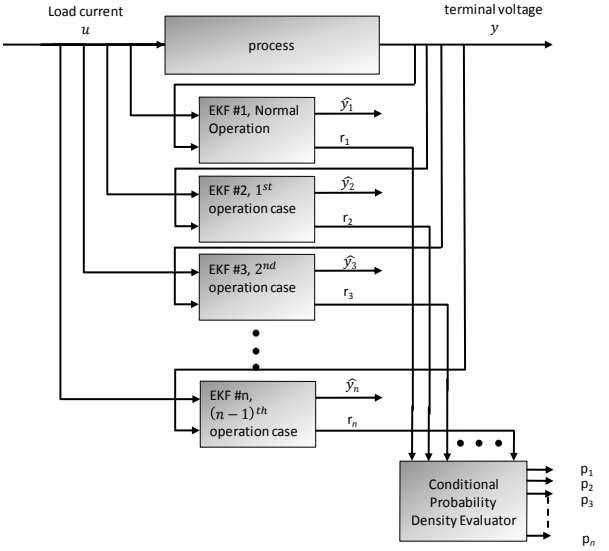

Fig. 3. Multiple-model residual generation and probability evaluation

In the next section, extended Kalman filters are introduced and used to estimate the terminal voltage and hence generate the residuals.

5. STATE ESTIMATION AND PROBABILITIES

5.1 Extended Kalman Filter Design

The extended Kalman filter is used for estimating the states of the non-linear battery model by linearizing around the current mean and covariance. For the non-linear system given by (9), (12) and (13), the discrete time extended Kalman filter (Anderson, 1979, Welch and Bishop, 2006, Fei

et al., 2008) estimates the non-accessible states of the Li-ion battery. The prediction equations are given by

$$\begin{aligned} \hat{x}(k \mid k-1) &= g(\hat{x}(k-1 \mid k-1), I_L(k-1)) \\ P(k \mid k-1) &= F(k-1)P(k-1 \mid k-1)F(k-1)^T + Q(k-1) \end{aligned} \quad (21)$$

where $\hat{x}(k \mid k-1)$ is the predicted state based on function g and evaluated at the estimated state and inputs available at sample k-1, $P(k|k$-1) is the predicted covariance estimate.

The recursive equations are given by

$$\begin{aligned} K(k) &= P(k \mid k-1)H(k)^T \left(H(k)P(k \mid k-1)H(k)^T + R(k)\right)^{-1} \\ \hat{x}(k \mid k) &= \hat{x}(k \mid k-1) + K(k)(z(k) - h(\hat{x}(k \mid k-1))) \\ P(k \mid k) &= (I - K(k)H(k))P(k \mid k-1) \end{aligned} \quad (22)$$

where $K(k)$ is the Kalman gain, $\hat{x}(k \mid k)$ is the updated state estimate, $P(k|k)$ is the updated covariance update, and $F(k$-$1)$ and $H(k)$ are the state transition and observation matrices respectively and given by

$$F(k-1) = \left.\frac{\partial f}{\partial x}\right|_{\hat{x}(k-1|k-1), I(k-1)} \quad \text{and} \quad H(k) = \left.\frac{\partial h}{\partial x}\right|_{\hat{x}(k|k-1), I(k-1)}$$

The estimated output is given by

$$\hat{y}(k) = h(\hat{x}(k \mid k), I_L(k)) \quad (23)$$

The residual signal for each model are obtained from the estimated output given by (23) and the measured terminal voltage $z(k)$ and is given by

$$r = z(k) - \hat{y}(k) \quad (24)$$

5.2 Conditional probability density evaluation

To generate accurate probabilities, the residuals are continuously monitored by the conditional probability density evaluation function. If the output of any model matches with the process measurement, the mean value of the residual signal goes to zero. The covariance of the residual signal evaluated at each sample is given by (Hanlon and Maybeck, 2000, Izadian and Famouri, 2010, Izadian, To appear, 2013, Izadian et al., 2009)

$$\psi(k) = C(k)P(k \mid k)C(k)^T + R \text{,} \quad (25)$$

where $C(k) = \left.\frac{\partial h}{\partial x}\right|_{\hat{x}(k|k)}$ is the system output vector which is linearized at the current state estimate. Considering a history of measurements $Z(k-1) = \left[z^T(1) \quad \ldots \quad z^T(k-1)\right]$, the conditional probability function can be given by

$$f_{z(k)|a,Z(k-1)}(z(k) \mid a, Z(k-1)) = \beta \exp(\bullet) \quad (26)$$

where

$$\beta = \frac{1}{(2\pi)^{l/2} |\psi(k)|^{1/2}} \quad (27)$$

l=1 is the measurement dimension, and

$$(\bullet) = -\frac{1}{2} r^T(k)\psi(k)^{-1} r(k) \quad (28)$$

The conditional probability evaluation for the nth model is then given by

$$p_n(k) = \frac{f_{z(k)|a,Z(k-1)}(z(k) \mid a, Z(k-1))p_n(k-1)}{\sum_{j=1}^{n} f_{z(k)|a,Z(k-1)}(z(k) \mid a, Z(k-1))p_j(k-1)} \quad (29)$$

where p_j is the conditional probability of j^{th} model, where j=1,…,n. The largest conditional probability amongst all is used as an indicator of the respective operating condition being true.

6. DESIGN OF EXPERIMENTS

The Li-ion battery selected for this study was A123 18650 $LiFePO_4$ single cylindrical cell (Systems, 2009). The schematic of the test setup for cycling and data acquisition of the Li-ion battery is shown in Figure 4.

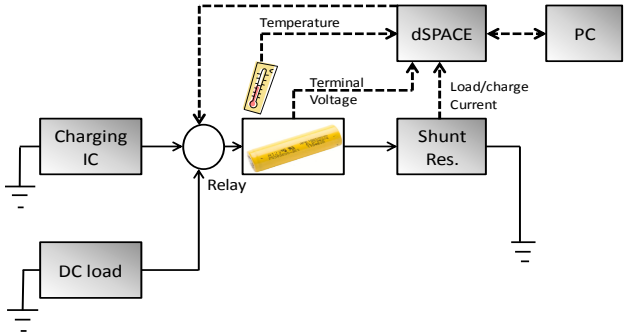

Fig. 4. Li-ion battery testing setup

The controlled discharging and charging of the battery is carried out by using a DC load and MCP73123/223 (Inc., 2013) $LiFePO_4$ charging IC respectively. The key battery parameters of terminal voltage, load/charge current and the skin temperature are recorded continuously. For this study, a brand new Li-ion battery under test was over discharged in a cyclic fashion. The over discharge regime is adopted from (Navy, 2004), where the Li-ion battery is discharged at maximum suitable discharge rate for 1.25 times the rated capacity of 18650 $LiFePO_4$ battery under test. The charging of the battery is carried out using a standard non-abusive charge regime. The battery is cycled 25 times using this discharge-charge regime and the critical battery parameters are continuously monitored.

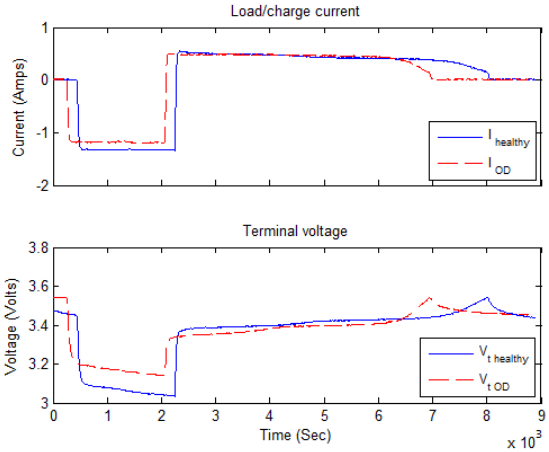

Fig. 5. Current and voltage profiles for healthy and OD battery

For the purpose of system identification, a standard discharge current is applied to the battery for partial SOC drop and the battery is charged again to full SOC. The typical noise filtered discharge-charge current and voltage curves are as shown in Figure 5.

Based on the current and voltage data of Figure 5, the parameter values for the healthy cell before and after the OD

cycles are estimated. The identified system parameters are given in Table I.

Table I. PARAMETER IDENTIFICATION DATA UNDER OVER DISCHARGE

Parameter	New battery	OD cycled battery
a_9	0.49161	0.748268
a_8	-0.08717	-0.07862
a_7	-0.32599	-0.42834
a_6	-0.27117	-0.37816
a_5	-0.03456	-0.08725
a_4	0.198062	0.201331
a_3	0.206745	0.219284
a_2	-0.07741	-0.10596
a_1	-0.00024	-0.03705
a_0	3.3558	3.490569
R_b	-0.06492	-0.05705
A_1	0.241634	0.607614
B_1	-0.06881	-0.06389
A_2	0.241634	0.034997
B_2	-0.06881	-0.06389

Using the identified system parameters, different operational models for healthy and OD cycled battery can be formulated. To mimic the actual operation of battery, a suitably scaled UDDS drive cycle, derived from AUTONOMIE (laboratory, 2010), is selected as an input to the fault detection system. The duration of test is 142 seconds and is obtained by running two cycles of UDDS consecutively; the current and corresponding voltage profiles are as shown in Figure 6.

Within the fault detection framework, both the extended Kalman filters access the same load current and terminal voltage measurements. Based on these signals the model states are estimated, terminal voltage is evaluated and the residuals are generated.

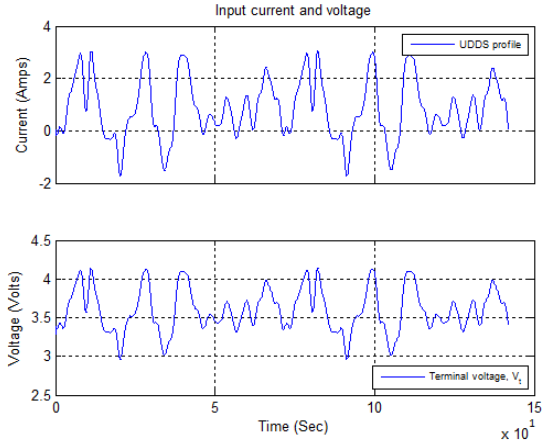

Fig. 6. UDDS load/charge current and terminal voltage profile

The initial state of the system is given by $[0.7\ 0\ 0]^T$, which implies 70% SOC and zero polarization voltages.

7. FAULT DETECTION PERFORMANCE

To test the effectiveness of the fault detection setup, a scenario representing the healthy and OD battery condition is created. The total simulation time is 142 seconds, from which healthy battery operation is simulated for the first 47.3 seconds. The OD battery operation is simulated from 47.4 to 94.6 seconds and finally healthy battery operation again from 94.7 to 142 seconds. Once the operational condition is diagnosed correctly, this setup helps to check the effectiveness of the fault detection algorithm to de-latch itself from its earlier diagnosis (Izadian and Famouri, 2010).

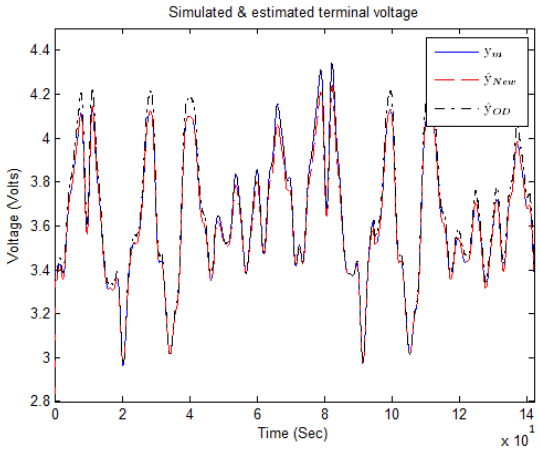

Fig. 7. Simulated and estimated terminal voltages

At every sample, the terminal voltages are estimated based on the measurement of current and terminal voltage. The simulated terminal voltage measurement $\hat{y}_m$ and the estimated terminal voltages from the new battery $\hat{y}_{new}$ and OD battery $\hat{y}_{OD}$ are shown in Figure 7. During the first 47.3 seconds, $\hat{y}_{new}$ matches while $\hat{y}_{OD}$ shows clear deviation from the simulated measurement. From 47.4 to 94.6 seconds, $\hat{y}_{new}$ deviates from the simulated measurement while $\hat{y}_{OD}$ shows good agreement. Finally, from 94.7 to 142 seconds, $\hat{y}_{new}$ again shows good match with the simulated measurement while $\hat{y}_{OD}$ shows deviation.

From Figure 8, the variation of the residuals along with the dependent probabilities can be observed, where P_{new} represents the probability of healthy operation of the cell and P_{OD} indicates the probability of OD operational condition. The OD operational condition was inserted at 47.3 seconds, as indicated by P_{OD}, when it transitions from 0 to 1. At the same time, P_{new} drops down to 0, thus indicating the battery operation is no longer healthy. At 94.6 seconds, the healthy operational condition is indicated with P_{new} transitioning from 0 to 1and P_{OD} dropping to zero.

The system residuals play an important role in accurate Li-ion battery condition detection and monitoring. When the process response matches with the estimated output from the filter, the mean value of the residual signal goes to zero, as observed in Figure 8. To demonstrate the effectiveness of model based battery fault diagnosis technique, the estimated parameter models are used in this validation. The purpose is to show the effectiveness of the technique in detecting the condition of the battery. As a next step, independent battery condition data can be used along with additional battery condition models for conducting experimental validation studies.

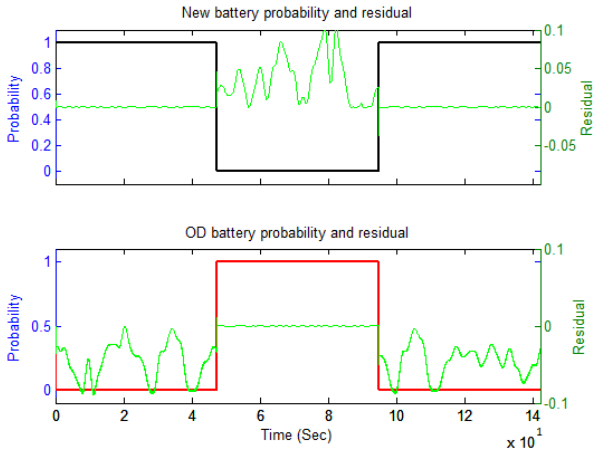

Fig. 8. Conditional probability density and residuals evaluated for new and OD battery condition

In some cases the results of Figure. 8 may not match as closely, but the relative degree of match will be sufficient to predict the battery condition accurately.

CONCLUSION

In this paper an observer based fault detection technique for Li-ion battery cell is developed. Experimental data from healthy and OD cycled battery is used to develop nonlinear system models. Extended Kalman filters are used to access the internal dynamics of the battery cell and estimate the condition of the system. The effectiveness of the fault detection is shown by its ability to capture small deviation from normal cell operation in real time.

REFERENCES

ABU-SHARKH, S. & DOERFFEL, D. 2004. Rapid test and non-linear model characterisation of solid-state lithium-ion batteries. *Journal of Power Sources,* 130**,** 266-274.

ALAVI, S. M., SAMADI, M. F. & SAIF, M. 2013. Diagnostics in Lithium-Ion Batteries: Challenging Issues and Recent Achievements. *Integration of Practice-Oriented Knowledge Technology: Trends and Prospectives.* Springer.

ANDERSON, B. D. O. 1979. Optimal filtering. *In:* MOORE, J. B. (ed.). Englewood Cliffs, N.J. :: Prentice-Hall.

BARSOUKOV, E. & MACDONALD, J. R. 2005. *Impedance Spectroscopy: Theory, Experiment, and Applications*, Wiley.

BULLER, S., THELE, M., DE DONCKER, R. W. A. A. & KARDEN, E. 2005. Impedance-based simulation models of supercapacitors and Li-ion batteries for power electronic applications. *Industry Applications, IEEE Transactions on,* 41**,** 742-747.

CHEN, W., CHEN, W. T., SAIF, M., LI, M. F. & WU, H. 2013. Simultaneous Fault Isolation and Estimation of Lithium-Ion Batteries via Synthesized Design of Luenberger and Learning Observers. *Control Systems Technology, IEEE Transactions on,* PP**,** 1-1.

EHSANI, M., GAO, Y. & EMADI, A. 2009. *Modern Electric, Hybrid Electric, and Fuel Cell Vehicles: Fundamentals, Theory, and Design, Second Edition*, Taylor & Francis.

FEI, Z., GUANGJUN, L. & LIJIN, F. A battery State of Charge estimation method with extended Kalman filter. Advanced Intelligent Mechatronics, 2008. AIM 2008. IEEE/ASME International Conference on, 2-5 July 2008 2008. 1008-1013.

HANLON, P. D. & MAYBECK, P. S. 2000. Multiple-model adaptive estimation using a residual correlation Kalman filter bank. *Aerospace and Electronic Systems, IEEE Transactions on,* 36**,** 393-406.

INC., M. T. 2013. MCP73123/223: Lithium Iron Phosphate ($LiFePO_4$) Battery Charge Management Controller with Input Overvoltage Protection. 2/11/2013 ed.: Microchip Technology Inc.

IOANNOU, P. & FIDAN, B. 2006. *Adaptive Control Tutorial*, Society for Industrial and Applied Mathematics.

IZADIAN, A. To appear, 2013. Self-Tuning Fault Diagnosis of MEMS. *International Federation on Automatic Control, Journal of Mechatronics*.

IZADIAN, A. & FAMOURI, P. 2010. Fault Diagnosis of MEMS Lateral Comb Resonators Using Multiple-Model Adaptive Estimators. *Control Systems Technology, IEEE Transactions on,* 18**,** 1233-1240.

IZADIAN, A., KHAYYER, P. & FAMOURI, P. 2009. Fault Diagnosis of Time-Varying Parameter Systems With Application in MEMS LCRs. *Industrial Electronics, IEEE Transactions on,* 56**,** 973-978.

KANEVSKII, L. S. & DUBASOVA, V. S. 2005. Degradation of lithium-ion batteries and how to fight it: A review. *Russian Journal of Electrochemistry,* 41**,** 1-16.

KAYPMAZ, T. C. & TUNCAY, R. N. An advanced cell model for diagnosing faults in operation of Li-ion Polymer batteries. Vehicle Power and Propulsion Conference (VPPC), 2011 IEEE, 6-9 Sept. 2011 2011. 1-5.

LABORATORY, A. N. 2010. AUTONOMIE. Argonne National laboratory.

NAGATA, M., SARASWAT, A., NAKAHARA, H., YUMOTO, H., SKINLO, D. M., TAKEYA, K. & TSUKAMOTO, H. 2005. Miniature pin-type lithium batteries for medical applications. *Journal of Power Sources,* 146**,** 762-765.

NAVY, D. O. T. 2004. Technical Manual For Batteries, Navy Lithium Safety Program Responsibilities And Procedures.

OGATA, K. 1995. *Discrete-time control systems,* Englewood Cliffs, N.J., Prentice Hall.

ORAZEM, M. E. & TRIBOLLET, B. 2008. *Electrochemical Impedance Spectroscopy*, John Wiley & Sons, Inc.

ROSS, S. M. 2010. *A first course in probability*, Pearson Prentice Hall.

SINGH, A., IZADIAN, A. & ANWAR, S. in press. Fault Diagnosis of Li-Ion Batteries Using Multiple-Model Adaptive Estimation. *IEEE Industrial Electronics, IECON 2013 - 39th Annual Conference on.* Vienna, Austria: IEEE.

SYSTEMS, A. 2009. *High Power Li-Ion APR18650* [Online]. Watertown, MA. Available: www.cosmoenergy.com/APR18650M1A_Datasheet_2009.pdf [Accessed 9/9/12 2012].

TARASCON, J. M. & ARMAND, M. 2001. Issues and challenges facing rechargeable lithium batteries. *Nature,* 414**,** 359-67.

WELCH, G. & BISHOP, G. 2006. An Introduction to the Kalman Filter. 2012. Available: www.cs.unc.edu/~welch/media/pdf/kalman_intro.pdf [Accessed 7/12/12].

XIDONG, T., XIAOFENG, M., JIAN, L. & KOCH, B. Li-ion battery parameter estimation for state of charge. American Control Conference (ACC), 2011, June 29 2011-July 1 2011 2011. 941-946.

ZHANG, J. & LEE, J. 2011. A review on prognostics and health monitoring of Li-ion battery. *Journal of Power Sources,* 196**,** 6007-6014.